Mineral and Redox Controls on Soil Carbon Cycling in Seasonally Flooded Soils

MINERAL AND REDOX CONTROLS ON SOIL CARBON CYCLING IN SEASONALLY FLOODED SOILS

A Thesis Presented

By

RACHELLE E. LACROIX

Submitted to the Graduate School of the
University of Massachusetts Amherst in partial fulfillment
of the requirements for the degree of

MASTER OF SCIENCE

September 2018

Plant and Soil Sciences

MINERAL AND REDOX CONTROLS ON SOIL CARBON CYCLING IN SEASONALLY FLOODED SOILS

A Thesis Presented

By

RACHELLE E. LACROIX

Approved as to style and content by:

_____
Marco Keiluweit, Chair

_____
Baoshan Xing, Member

_____
Justin Richardson, Member

_____
Wesley Autio, Department Head
Stockbridge School of Agriculture

ACKNOWLEDGEMENTS

I would like to thank my advisor Marco Keiluweit and my committee members Baoshan Xing and Justin Richardson for their support in my project. I would also like to thank Mickey Spokas for her support and encouragement for me to pursue soil science. Additionally, I thank my lab members Mariela Garcia Arredondo, Morris Jones, and Carolyn Anderson for their help and inspiration. A large portion of my project would also not have been possible without the dedication and help of Menli McCreight and Michael Lupario. Lastly, I would like to thank the beamline scientists from the Canadian Light Source, Jay Dynes and Tom Regier, and Malak Tfaily from the Environmental Molecular Science Laboratory for all their technical support.

ABSTRACT

MINERAL AND REDOX CONTROLS ON SOIL CARBON CYCLING IN SEASONALLY FLOODED SOILS

SEPTEMBER 2018

RACHELLE E. LACROIX, B.S., UNIVERSITY OF MASSACHUSETTS AMHERST

M.S., UNIVERSITY OF MASSACHUSETTS AMHERST

Directed by: Professor Marco Keiluweit

Soils contain nearly three times the amount of carbon (C) than the atmosphere, with C turnover times ranging from centuries to millennia. Although wetland soils represent a relatively small portion of the terrestrial landscape, they account for an estimated 20-30% of the global C reservoir. Seasonally flooded soils are likely the most vulnerable wetlands to climate change, as changing temperature and precipitation patterns are expected to alter the timing and duration of flooding. Seasonal variations in soil moisture are recognized as a critical control on soil C stocks and CO_2 emissions. However, the relative influence of associated changes in soil oxygen availability, root dynamics and the stability of mineral-organic associations are largely unknown. The overarching goal of this study was to examine the relative influence of redox state, root density and mineralogy on C cycling

within seasonally flooded soil. To accomplish this goal, we combined seasonal monitoring of soil moisture, redox potential, and carbon dioxide emissions with a characterization of organic matter composition, mineralogy and root biomass along upland to lowland transects. We found that water saturation was the limiting factor for CO_2 emissions from seasonal flooded lowland soils, whereas soil temperature primarily regulated emissions from upland soils. Seasonal water saturation also resulted in topsoil C accumulation in lowlands compared to uplands, despite experiencing prolonged aerobic periods. Moreover, the C that accumulated in lowland topsoils was more chemically reduced compared to upland soils. However, the C chemistry in the subsoil showed the opposite trend of being more reduced in uplands compared to lowland subsoils. In sum, our results suggest that anaerobically protected soil C in seasonal flooded soils is particularly vulnerable to changing moisture regimes in response to climate change. To what extent this expected C loss is compensated by upland plant encroachment, or the neoformation of mineral-organic associations, warrants future research.

TABLE OF CONTENTS

Page

LIST OF TABLES

LIST OF FIGURES

CHAPTER 1

INTRODUCTION

Although wetland soils cover a relatively small portion of the Earth's land surface, they store an estimated 2-30% of the global soil C stocks (Mitsch et al., 2012). However, this C pool is under pressure from climate change, with increasing severity and frequency of droughts having substantial, yet largely unresolved consequences (Ise et al., 2008, Brooks et al., 2009, Fenner and Freeman, 2011). The expected droughts in wetlands are expected to release previously stored C back into the atmosphere (Gorham et al., 1991; Moore et al., 1998; Chmura et al., 2003). Prior studies focused on C cycling in wetland soils have been primarily aimed at organic wetlands, such as peats and bogs (Moore and Knowles, 1989; Laine et al., 1996; Trettin et al., 2005; Dinsmore et al., 2009) or coastal wetlands (Kirwan and Blum, 2011; Kraus et al., 2012; Miao et al., 2013; Chen et al., 2015). In comparison, freshwater mineral wetland soils have received less attention though they are estimated to contain 46 Pg C globally (Bridgham et al., 2006, Fissore et al., 2009).

Previous studies on C cycling in mineral wetland soils are limited to permanently flooded, rather than seasonally flooded sites (Krauss and Whitbeck, 2012; Brooker et al., 2014). Yet the consequences of climate change will likely be most immediately evident in seasonal wetlands due to their dependence upon precipitation and seasonal groundwater recharge during the non-growing season (Erwin, 2009). Seasonal wetlands can be considered as early warning and detection ecosystems; forecasting the impacts of climate change on permanently flooded mineral wetlands. Thus, seasonally flooded wetlands are

ideal model ecosystems to study the effects of climate change on larger permanently flooded wetland soils (Brooks, 2009).

Seasonal wetlands are geomorphic depressions in the landscape that have distinct hydrologic phases of flooding and draining (Zedler, 2003). These ephemeral wetlands are small (<1 hectare), but ubiquitous – comprising nearly 70% of all temperate forest wetlands in the US (Tiner, 2002; Brooks, 2004). Seasonal flooding and drainage not only creates biogeochemical "hotspots" for soil C and nutrient cycling along upland-to-lowland transitions, but also "hot moments" as these transition zones move seasonally (Capps et al., 2014; Marton et al., 2015). These transition zones are also relatively large, as the generally small size of seasonal wetlands results in a disproportionally large and dynamic terrestrial-aquatic interface relative to total wetland area (Cohen et al., 2016). Determining the controls on C cycling within seasonally flooded mineral soils thus requires specific consideration of the fluxes and dynamics across these terrestrial-aquatic transitions.

Though temperature and soil moisture are principle controls on C cycling in soils generally (Lloyd and Taylor, 1994; Davidson and Janssens, 2006; Wang et al., 2014), water saturation is a critically driver of soil organic matter (OM) decomposition processes in seasonally flooded systems (Neckles and Niell, 1994). Water saturation governs oxygen availability in soil pore spaces, as oxygen diffusion in water is 10,000 times slower than in air (Letey, 1964; Colmer, 2003). Oxygen depletion occurs rapidly in saturated soils causing redox potentials to decline. Low oxygen concentrations inhibit microbial activity (Freeman et al., 2001) and reduces production (Hall and Silver, 2014) of oxidative enzymes catalyzing OM depolymerization. Once oxygen is depleted, microbes rely on alternative terminal electron acceptors (NO_3^-, Mn^{4+}, Fe^{3+}, SO_4^2) in heterotrophic respiration pathways

that yield less energy (Sutton-Grier et al., 2011). These thermodynamic constraints also dictate the types of organic substrate microbes are able to use in heterotrophic respiration. Anaerobic conditions limit microbes to substrates that are chemically more oxidized, in turn preferentially preserving more chemically-reduced organic compounds in soils and sediments (Boye et al. 2017; Keiluweit et al., 2017). While CO_2 emissions are often correlated with soil redox potential (Silvola et al., 1996; Chen et al., 2018; Koh et al., 2009; Liu et al., 2013), it is unclear to what extent such metabolic constraints result in the selective preservation of chemically reduced organic compounds in seasonally flooded systems where soils are fully oxygenated for prolonged periods.

Water saturation also impacts soil by controlling vegetation type and density – thus acting as an indirect control on root growth and activity belowground. Roots contribute to soil C stocks through active rhizodeposition (exudates, secretions, dead border cells, and mucilages), dead root residues (Jones et al., 2009), and root-associated microbes (Bradford et al., 2013). Roots are the main contributors to C stocks in upland soils (Rasse et al., 2005; Hu et al., 2015), but root contributions to soil C stocks in wetlands is less clear. Water saturation directly inhibits root growth due to the associated the low redox potentials (Drew and Lynch, 1980; Day and Megonigal, 1993; Tokarz and Urban, 2015; Pezeshki and DeLaune, 2012). Indirectly, water saturation in soil selects for plant species that can tolerate water stress – typically species that have developed advantageous traits to survive flooded conditions, such as shallow rooting systems (Pezeshki, 2001). However, seasonally flooded soils select for an even smaller niche of plants, as they must be tolerant of both upland and lowland conditions (Palik et al., 2007). How these facultative upland-to-

lowland plant species contribute to soil C stocks through root inputs in seasonal wetlands is still not clear.

In addition to restricting microbial metabolism and root growth, water saturation also influences the concentration and distribution of redox-active metals (Wilson et al., 2013). In upland soils, iron (Fe) or aluminum (Al) (hydr)oxides protect OM from microbial decomposition, thereby contributing to C storage for centuries to millennia (Torn et al., 1997; Wagai and Mayer, 2007). In flooded soils, however, the rapid depletion of oxygen upon flooding can result in the reductive dissolution of Fe(III) oxides (Munch and Ottow, 1983; Madigan et al., 1984), potentially causing the mobilization of previously Fe-bound OM (Hall et al., 2016). During water table drawdown, Fe(II) may be leached from the profile or re-oxidized to Fe(III) oxides upon re-oxygenation of soil pores (Wang et al., 2016). While redox-mediated transformations and export of Fe oxides is a well-known phenomenon ("gleying") in seasonally flooded soils (Bouma, 1983; D'Amore et al., 2004), their impact on mineral-associated C pools has yet to be determined. Further, Al oxides, rather than Fe oxides, are the predominate mineral phases contributing to OM retention in forested floodplain sediments because their solubility is controlled by pH rather than redox conditions (Darke and Walbridge, 2000), and may thus play a critical role in mineral protection in seasonally flooded soils.

Water saturation likely governs C cycling in seasonally flooded soils through its impact on microbial metabolic constraints, root dynamics and mineral protection; but how the relative contribution of these biogeochemical controls vary across spatial and temporal gradients is still unknown. A recent study along hillslope transects in tropical forest soils

representing an oxygen gradient (Hall and Silver, 2015), for example, found that a combination of Fe (II) (a proxy for reducing conditions), fine root biomass, and total Fe and Al concentrations explained the most variation of surface soil C contents. How the relationships between C and important biogeochemical controls differ in systems that undergo longer, yet not permanent, periods of water saturation is still in question – especially with depth.

In this study, we aimed to identify the predominant environmental and biogeochemical controls on CO_2 efflux, C content, and OM composition in seasonally flooded mineral soils. To accomplish this goal, we studied the impact of seasonal flooding on C cycling in six replicated upland-to-lowland transects in forested mineral wetlands typical for the Northeastern US (Brooks, 2004). Our objectives were to (i) identify the environmental parameters that drive temporal dynamics of CO_2 efflux in seasonally flooded soils and (ii) examine the relative importance of biogeochemical controls on C concentration and C chemistry with depth. To accomplish our first objective, we related soil CO_2 efflux at three landscape positions spanning the transect (upland, transition, and lowland) over the course of a full drainage and flooding cycle to measures of soil temperature, moisture, water table depth and redox potential. To accomplish our second objective, we examined variations in C content and C chemistry (composition of OM compounds and C functional group) across the in both surface and subsurface horizons (down to an average of one m depth) in relation to biogeochemical factors (root biomass, clay content, and extractable metals).

We hypothesized that (i) soil redox conditions, alongside soil temperature, are the dominant control of CO_2 emissions in seasonally flooded lowland soils, (ii) seasonally

reduced lowland soils will have lower capacities for mineral-organic associations than upland soils, and (iii) water saturation and the associated low redox potentials in wetlands will preferentially select for the accumulation of chemically-reduced OM compounds.

CHAPTER 2

METHODS

2.1 Site Description

Our study included six replicate forested wetlands in western Massachusetts that experience seasonal flooding; three sites are located at the UMass Experimental Farm Station in South Deerfield, MA, and three located within the Plum Brook Conservation area in South Amherst, MA. All sites consisted of soils that are glacially-derived sandy loams classified as mesic Typic Dystrochrepts. Vegetation is dominated by red maple (*Acer rubrum*) and white oak (*Quercus alba*) stands with understory vegetation primarily composed of cinnamon fern (*Osmunda cinnamonea),* Canada mayflower (*Maianthemum canadense),* reed canary grass (*Phalaris arundinacea*), and jewelweed (*Impatiens capensis).* Mean annual air temperatures ranged from 3 to 15 ^{o}C and mean annual precipitation (rainfall and snowfall) is between 91 and 180 cm (National Centers for Environmental Information (NCEI), National Oceanic and Atmospheric Administration (NOAA).

2.2 Field Measurements

A transect in each seasonal wetland was delineated from an upland position to a lowland position. Three positions, termed “upland”, "transition”, and “lowland”, along each transect were established as monitoring stations and for soil sample collection. We used water table fluctuation data from a prior study (Collins, K. 2013, UMass thesis) to describe moisture conditions at each landscape position. The upland position is in a

forested landscape, approximately five meters away from the edge of the wetland, and does not undergo any flooding. The transition position is located on the edge of the wetland, which typically does not get flooded in an average rainfall year, but is under the influence of water table rise. The lowland position is in the lowest point of the wetland and is flooded for several months throughout the year. Horizons in the upland position were classified as A (0-25 cm), B (25-55 cm), and C (55-84+ cm) horizons; in the transition position as A (0-28 cm), C (28-48 cm), and Cg (48-69+); and in the lowland position as A (0-25 cm), C (25-35 cm), and Cg (35-68+ cm) (Soil Survey Staff 1999). Each landscape position was monitored for CO_2 emissions, soil temperature, volumetric moisture content (VMC) at 0 to 10 cm, water table depth, and E_h. Field measurements were collected weekly at each designated landscape position in all six seasonal wetlands from May through August, then monthly from September through April. A field portable automated gas flux analyzer (LI-8100A, LI-COR Biotechnology, Lincoln, NE) was used to measure rates of CO_2 emissions, on permanently installed PVC collars, soil temperature and VMC. Three measurements of CO_2 fluxes were taken at each individual PVC collar using observation times of one minute, with 15 second dead band and pre- and post- purge times. The standard deviation of three observations was calculated in the field and a 15 % threshold was used for acceptable measurements. If the resulting standard deviation of the three measurements was greater than 15 % subsequent measurements were taken until the threshold was met. Water table fluctuations were monitored using slotted PVC pipes installed to depths of 100 cm. Platinum-tipped E_h probes were installed in triplicate at each depth of 15-, 30-, and 45-cm; each group (nine) of E_h probes were accompanied with a single salt bridge filled with saturated KCl in 3% agar for the reference electrode. In total, each landscape position had

18 redox probes installed at each depth. E_h was measured using a calomel electrode (Fisher Scientific, Pittsburg, PA) attached to a voltmeter (Radio Shack, Fort Worth, TX) and corrected to a standard hydrogen electrode by adding 244 mV to each reading (Bates, 1973, Fielder et al., 2007).

2.3 Soil Sampling and Analyses

Soil samples were collected from all sites, positions and horizons using hand-augers. Coarse rocks and roots were removed from soil samples which were then sieved using standard 2 mm screens. Particle size distribution was determined using the pipette method outlined by Gee and Bauder (1986). Total C and N were determined with an elemental analyzer (Hedges and Stern, 1984). Extractable iron and aluminum concentrations were measured on each soil horizon from all three positions from the six pools (n=62) using ammonium-oxalate and citrate-bicarbonate-dithionite (CBD) extraction procedures (Loeppert and Inskeep, 1996). Ammonium-oxalate extractable Fe (Fe_o) and Al (Al_o) represent the poorly crystalline pool of Fe, while the CBD extractable Fe (Fe_d) and Al (Al_d) represent the total reducible Fe.

Root biomass was determined by taking soil cores in all six wetlands at each position along the designated moisture transects. The cores were taken at 0-20cm, 20-40cm, and >40cm Root biomass was determined using a USDA hand sieving method (National Soil Survey Center). The initial values of root biomass were used to determine biomass values for each soil horizon using an equal-area quadratic spline function (Spline Tool v2.0, ASRIS). Mean E_h values for each soil horizon were also estimated using the spline function.

2.4 Carbon 1s Near-edge X-ray Absorption Fine Structure (NEXAFS) Spectroscopy

To determine the relative abundance of specific C functional groups and degree of oxidation, soil samples were analyzed using C (1s) near edge X-ray absorption fine structure (NEXAFS) spectroscopy at the Canadian Light Source (CLS) in Saskatoon, Canada. Soil samples from individual horizons were gently ground, slurried in DI-H_2O and pipetted onto clean In foils. After drying, C NEXAFS spectra were obtained using the spherical grating monochromator (SGM) beamline 11ID-1 (Regier, 2007). Step scan mode (0.25 eV steps from 270 to 320 eV) was used to minimize x-ray damage. A dwell time of 20 ms was used between scans. Individual spectra were collected at new locations on each sample for a total of 40 to 60 scans. The beamline exit slit was set at 25 mm, and the fluorescence yield data was collected using a two-stage microchannel plate detector. The resulting spectra were averaged for each sample and the averaged spectrum was then baseline normalized to zero and then normalized the beamline photon flux (I_o) from a separate Au reference foil. Each spectrum was calibrated to the carboxylic acid peak (288.5 eV) of a citric acid standard. Pre-edge (270-278 eV) and post-edge (310-320 eV) and an E_0 (290 eV) values were used to perform an edge step normalization. Peak deconvolution was conducted in Athena (Demeter version 0.9.25, 2006-2016); Ravel and Newville 2005) to determine the relative abundances of functional groups; namely carboxylic and amine C, aromatic C and aliphatic C. Positions of peaks were assigned energies reported by Schumacher at al. (2006) and Soloman et al. (2005). Gaussian peak positions, their full-width at half-maximum, and the arc tangent function were fixed. Peak magnitude was set to vary freely during the fitting process. Parameters were adjusted until optimal fits for each spectrum were achieved and all spectra were fitted with these final parameters.

2.5 Fourier-transform Ion Cyclotron Resonance Mass Spectrometry (FT-ICR-MS)

To determine the composition of bioavailable compounds that can potentially be used in microbial respiration (<600Da, Logue et al., 2016), water extracts of soil samples were collected on a 12 Tesla Bruker SolariX Fourier-transform ion cyclotron resonance mass spectrometer located at Environmental Molecular Sciences Laboratory (EMSL), a Department of Energy Biological and Environmental Research (DOE-BER) national user facility located in Richland, WA. Soil samples were extracted with ultrapure DI-H_2O using one gram of soil and 10 mL of DI-H_2O (1:10). The samples were sealed in 15 mL conical tip tubes and shaken for one hour. Samples were then centrifuged and filtered using syringe-filters and the resulting filtrate solution was used for FT-ICR-MS analysis. A standard Bruker electrospray ionization (ESI) source was used to generate negatively charged molecular ions; samples were then introduced directly to the ESI source. The instrument was externally calibrated to a mass accuracy of <0.1 ppm weekly using a tuning solution from Agilent, which contains the following compounds: $C_2F_3O_2$, $C_6HF_9N_3O$, $C_{12}HF_{21}N_3O$, $C_{20}H_{18}F_{27}N_3O_8P_3$, and $C_{26}H_{18}F_{39}N_3O_8P_3$ with an m/z ranging between 112 to 1333. The instrument settings were optimized by tuning on a Suwannee River Fulvic Acid (SRFA)) standard. Blanks (HPLC grade MeOH) were also ran at the beginning and the end of the day to monitor potential carry over from one sample to another. The instrument was flushed between samples using a mixture of water and methanol. The ion accumulation time (IAT) was varied to account for differences in C concentration between samples and varied between 0.1 and 0.3 s. Ninety-six individual scans were averaged for each sample and internally calibrated using OM homologous series separated by 14 Da (–CH_2 groups).

The mass measurement accuracy was less than 1 ppm for singly charged ions across a broad m/z range (i.e. 200 <m/z <1200). To further reduce cumulative errors, all sample peak lists for the entire dataset were aligned to each other prior to formula assignment to eliminate possible mass shifts that would impact formula assignment. Putative chemical formulas were assigned using Formularity software (Tolić et al., 2017). Chemical formulas were assigned based on the following criteria: S/N >7, and mass measurement error <1 ppm, taking into consideration the presence of C, H, O, N, S and P and excluding other elements. Peaks with large mass ratios (m/z values >500 Da) often have multiple possible candidate formulas. These peaks were assigned formulas through propagation of CH_2, O, and H_2 homologous series. Additionally, to ensure consistent choice of molecular formula when multiple formula candidates are found the following rules were implemented: we consistently chose the formula with the lowest error with the lowest number of heteroatoms and the assignment of one phosphorus atom requires the presence of at least four oxygen atoms. Peaks that were present in the blanks were subtracted from the sample data sets. Additionally, all single peaks i.e. peaks that are present in only one sample were removed and are not included in the downstream analysis. To further identify only "unique" peaks, we compared samples with the same group against each other to keep the peaks in the sample set that occur at least half of the samples for that group; peaks that occurred in less than half the samples were discarded from the final data set.

To visualize differences in SOM composition, compounds were plotted on a van Krevelen diagram corresponding to their H/C (hydrogen to carbon) vs. O/C (oxygen to carbon) ratios (Kim et al., 2003). Van Krevelen diagrams provide a way to visualize and compare the average properties of OM and assign compounds to the major biochemical

classes (i.e., lipid-, protein-, lignin-, carbohydrate-, - and condensed aromatic-like) (Kim et al., 2003). Additionally, the nominal oxidation state of carbon (NOSC) was calculated (Keiluweit et al., (2017):

$$NOSC = - ((- Z + 4C + H - 3N - 2O + 5P - 2S)/ C) + 4 \quad (1)$$

in which C, H, N, O, P, and S correspond to stoichiometry values measured by FT-ICR-MS, and Z is equal to the net charge of the organic compound (assumed to be zero).

2.6 Statistical Analyses

All statistical analyses and plots were done using Rstudio (Version 1.0.136, R Core Team 2015), including linear regressions, correlation analyses, and FT-ICR-MS data resolution. Analysis of variance (ANOVA) and Tukey's post-hoc analyses were conducted in Rstudio; analyses were conducted on square root transformed data when assumptions of normal distribution were not met. Packages used include plotly (Sievert et al., 2017), multcompview (Graves et al., 2015), agricolae (Mendiburu 2017), plyr (Wickham 2016), ggplot2 (Wickham et al., 2016) and Hmisc (Harrell et al., 2018).

CHAPTER 3

RESULTS

3.1 Seasonal Dynamics

Although our positions along the upland to wetland transect (i.e., upland, transition, lowland) are only a few meters apart each, we found significant differences in the seasonal dynamics of soil respiration, water table depth, moisture content and redox conditions (Fig. 1).

3.1.1 Soil Respiration

CO_2 fluxes in each landscape position began to rise in May and peaked in September. Thereafter, CO_2 efflux in all positions gradually declined to a baseline level until November. CO_2 fluxes remained at that low baseline level through April (Fig 1a). Cumulative CO_2 emissions during the growing season substantially decreased across the upland-to-lowland transect (Table 1). Relative to the lowland position (24 mol CO_2 m^{-2} $year^{-1}$), cumulative CO_2 emissions were 38% greater in the transition position (33 mol CO_2 m^{-2} $year^{-1}$), and 58% greater in the upland position (38 mole CO_2 m^{-2}). This general difference became even more pronounced when cumulative CO_2 emissions were normalized to C content, with the upland position showing greater emissions than both the transition (p-value <0.001; Tukey's HSD) and lowland (p-value <0.001, Tukey's HSD) positions. In the non-growing season, the transition position registered the largest cumulative CO_2 flux (20 mole CO_2 m^{-2}), but there were no noticeable differences between the upland and lowland positions (16 and 15 mole CO_2 m^{-2}, respectively) (Table 1).

3.1.2 Water Table Dynamics

As typical in seasonal wetlands in the Northeastern US (Brooks, 2004), the water table in all three positions was highest from January to July and lowest from August through December (Fig. 1b). The lowland position had the greatest fluctuations in water table depth; the water table rose above the ground surface from February through June and dropped below the ground surface from July through January (-2 to -42 cm) (Table S1). The water table in the transition and upland positions showed similar seasonal dynamics, but was significantly lower than the lowland throughout the year.

3.1.3 Volumetric Moisture Content (VMC)

VMC generally followed water table fluctuations, although with less seasonal variation (Fig. 1c). Soil moisture was consistently the greatest in the lowland position; during the growing season VMC was 20% greater than the upland position (p-value < 0.05; Tukey's HSD), and 15% greater in the non-growing season (p-value < 0.05; Tukey's HSD) (Table S1).

3.1.4 Redox Potential

Redox potential (E_h) values typically mirrored the hydrologic conditions of each landscape position, with the lowest values generally occurring from May to July and the highest values between October and February (Fig. 1d). The lowland position had the largest seasonal amplitude, with values of less than 100 mV between May and July and above 500 mV from October to December. E_h in the transition position only fell to values between 200 to 300 mV between May and July, and recovered to values near 600 mV by October. The E_h values at the upland position remained above 450 mV throughout the

entire year at 15 cm depth, but reached 400 mV or lower at 30 and 45 cm depths from May to July.

3.2 Control on CO_2 Fluxes

To determine which of the above environmental parameters best predict soil respiration across the hydrological gradient, we conducted a series of regression analyses (Fig. 2a-d). Regression analyses were carried out for subsets of the data representing the (i) full year, (ii) growing season or (iii) non-growing season (Table 2).

3.2.1 Soil Temperature

The strength of the relationship between CO_2 flux and soil temperature, as expressed by how well the data can be described using the Arrhenius equation (Davidson et al., 2012; Sierra, 2012), decreased along the upland-to-lowland transect (Fig. 2a). Soil temperature explained the most variance of CO_2 fluxes in the upland positions throughout the full year ($r = 0.72$, $p < 0.001$) and the growing season ($r = 0.62$, $p < 0.001$) (Table 2). Comparing the three landscape positions, soil temperature explained the least variation of CO_2 fluxes in all cases in the lowland position, especially in the growing season ($r = 0.45$, $p < 0.001$).

3.2.2 Soil Moisture

As the relationship between CO_2 flux and soil temperature became weaker, that between CO_2 flux and water table depth gradually became stronger along upland-to-lowland transitions. CO_2 flux and water table depth (Fig. 2b) were significantly negatively correlated in the lowland positions in the full, growing season and non-growing season time periods (Table 2). The strongest correlation between water table depth and CO_2 flux

occurred in the lowland position during the growing season ($r = -0.55$, $p < 0.001$), where it had a stronger relationship with CO_2 flux than soil temperature. Similarly, VMC and CO_2 fluxes were negatively correlated in the lowland position ($r = -0.51$, $p < 0.001$), with VMC showing a stronger relationship with CO_2 flux than soil temperature during the growing season (Fig. 2c)

3.2.3 Soil Redox Potential

In keeping with a strong relationship between moisture and respiration at the transition and lowland positions, E_h was also most significantly correlated with CO_2 at the transition and lowland positions (Fig. 2d). E_h was a comparable predictor for CO_2 flux in both the lowland ($r = 0.40$, p-value <0.001) and transition ($r = 0.41$, p-value <0.001) positions during the growing season, but had no correlation with CO_2 flux in the upland position (Table 2). The strong correlations between E_h and CO_2 emissions were primarily limited to the lowland position.

In sum, CO_2 emissions in the upland position were most strongly correlated to soil temperature, while water table and VMC correlated more strongly with CO_2 fluxes in the lowland position during the growing season.

3.3 Distribution of C, Root Biomass, and Mineralogy

To identify how roots and mineralogy affected the distribution of C across the upland-to-lowland transect, we examined C concentrations in relation to root biomass, texture, extractable Fe and Al and E_h (Table 3).

3.3.1 Carbon Content

Along the upland-to-lowland transects, C concentrations in the surface horizons increased whereas concentrations in the subsurface horizons decreased along the transect (Table 3). C concentrations in the lowland position topsoil were two and four times greater than the transition (p-value < 0.01; Tukey's HSD) and upland positions subsoils (p-value < 0.001; Tukey's HSD), respectively. In contrast, the subsoils in the upland positions had nearly double the C concentrations than the subsoils of the transition and lowland positions.

3.3.2 Root Biomass

Root biomass significantly decreased from the upland to the lowland positions (Table 3). The upland position had nearly 10-times the amount of root biomass as the lowland position in the surface and subsurface horizons.

3.3.3 Mineralogy

Silt and clay content increased from the upland to the lowland positions, particularly in the subsoil (+33%, Table 3). Fe_o decreased by nearly 50 % from the upland to lowland positions in the topsoil. However, in the subsoil Fe_o almost doubled from the upland to the lowland positions. The upland position had significantly more Al_o than the transition and lowland positions in all horizons ($p < 0.001$, ANOVA), and declined with depth in each landscape position. Fe_d and Al_d strongly followed the trends of Fe_o and Al_o (Table 3), thus we further limit our discussion to Fe_o and Al_o.

3.4 Pairwise Relationships Between C And Biogeochemical Variables

To determine the relative influence of roots, mineralogy and redox conditions in each landscape position, we conducted pairwise comparisons between total C and root

biomass, silt and clay, Fe_o, Al_o or mean E_h in the growing season (Fig. 3a-e, Table 4). Root biomass and C were significantly correlated in the lowland ($r = 0.66$, p-value < 0.01), transition ($r = 0.72$, p-value < 0.001), and upland positions ($r = 0.59$, p-value < 0.001), even though root biomass in the lowland position was significantly less than that of the upland and transition positions (Fig 3d). Silt and clay contents showed no relationship with C in any landscape position (Fig 3a). Fe_o was positively correlated with C in the upland position ($r = 0.70$, p-value < 0.001), yet this relationship was not maintained in the transition and lowland positions. Al_o had the strongest correlation with C in the lowland position ($r = 0.84$, p-value < 0.001), and less so in the upland position ($r = 0.50$, p-value < 0.05) (Table 4). E_h was most strongly correlated with C in the upland position ($r = 0.32$, p-value > 0.05), but showed little relationship in the transition ($r = 0.10$, p-value > 0.05) and lowland ($r = 0.14$, p-value > 0.05). Analysis of the topsoil horizons of the three landscape positions together showed a significant relationship between E_h and C ($r = 0.48$, $p < 0.05$). However, in the subsoil, there was no significant correlation between E_h and C. The strength of linear regression relationships between C and biogeochemical co-variates differentiated by position (Fig. 3a-e; Table 4). In the lowland, Al_o and root biomass were the strongest and most significant covariates of C. In the transition position, root biomass was only significant correlated with C. In the upland, Fe_o, Al_o, and root biomass were all significantly associated with C concentrations.

3.5 C Chemistry Across Upland-to-Lowland Transitions

To determine oxidation state of C and origin of OM along upland-to-lowland transects, we analyzed the composition of solid-phase and water-extractable OM.

3.5.1 NEXAFS Spectroscopy of Bulk Samples

Analysis of bulk SOM spectra using C (1s) NEXAFS showed an overall increase in abundance of chemically-reduced OM from the upland to the lowland in the topsoil, but an opposite trend in the subsoil (Fig. 4a, Table S3). Aliphatic, aromatic and carboxylic and amide C relative abundances were significantly different amongst the three landscape positions (p-value = <0.05, ANOVA). The relative abundance of aliphatic and aromatic C increased from the upland to the lowland position in the surface horizons, but their contribution decreased along the same transect in the subsurface horizons. Carboxylic and amide C decreased in the surface horizons from upland to lowland, yet increased slightly in the subsoil along the same transect. On average, aliphatic and aromatic C decreased with depth, while carboxylic and amide and O-alkyl C increased with depth (Fig. 4a, Table S3).

As a measure of the degree of oxidation, we calculated carboxylic to aromatic C ratios (Fig. 4b). Across the transect in the topsoil, the ratio was lower in the lowland position than the upland position. In the subsoil, the ratio nearly doubled from the upland position's C-horizon to the lowland position's Cg-horizon. C NEXAFS functional group data showed an increase in aliphatic and aromatic C in the topsoil from upland to lowland transitions. Although in the subsoil, there was an apparent increase in carboxylic and amide C while aromatic and aliphatic C decreased.

3.5.2 FT-ICR-MS Analysis of Water Extracts

To assess changes in the oxidation state of smaller, bioavailable organic compounds that may be used in microbial respiration, water extracts of all sampled were analyzed by FT-

ICR-MS. In the topsoil, the average nominal oxidation state of carbon (NOSC) of the detected compounds decreased from the upland to the lowland positions. In the subsoil, however, NOSC increased along the same transect (Fig. 5b). Additionally, the average molecular weight of the detected compounds was greater in the lowland subsoils compared to the upland subsoils, but was lower in the lowland topsoil compared to the upland position (Fig. 5c). In the topsoil, lower NOSC values in the lowland position coincided with lower lignin and higher carbohydrate values when compared to the upland position (Fig 5a). The Cg-horizon in the lowland position had higher NOSC values which were concurrent with more lignin and tannin compounds and lower lipid amounts when compared to the C-horizon in the upland position (Fig. 5a). NOSC values decreased with depth in the upland and transition positions, however increased with depth in the lowland position. The decrease in NOSC in the upland position with depth was matched with an increase in lipids and decrease in tannins. The increase in NOSC in the lowland position with depth was in conjunction with an increase in lignin amounts and decline in carbohydrates (Fig. 5a).

CHAPTER 4

DISCUSSION

Our results show that the factors regulating CO_2 emissions and C accumulation shift along upland-to-lowland transects (Fig. 2). Cumulative CO_2 emissions, for the whole year, declined by nearly 25% from the upland to the lowland positions. This difference occurred primarily in the growing season, where emissions were 40% lower in the lowland position than the upland position (Table 1). Lower CO_2 emissions in the lowland position were consistent with 3.5-times more C in the A-horizon compared to the A-horizon in the upland position (Table 3). In addition to the accrual of C in the lowland topsoil, we found evidence of the selective preservation of chemically-reduced C compounds in the lowland surface soils compared to the upland positions (Fig. 4). Surprisingly, the subsoil horizons in the lowland positions had greater contributions of more chemically-oxidized C to the soil C pool, which illustrates how water saturation differentially impacts C cycling in deeper mineral soil horizons compared to surface soils. Combined, our results highlight how water saturation and reducing conditions control C inputs, chemical composition of C, and the capacity for mineral protection.

4.1 Environmental parameters controlling CO_2 emissions

Our hypothesis that reducing conditions inhibit microbial respiration and thus reduce CO_2 emissions in seasonally flooded soil is supported by our seasonal field data. We found strong correlations between seasonal CO_2 emissions and VMC, water table depth, and E_h in the seasonally flooded lowland positions of our study sites (Fig. 2). In the

upland position, however, soil temperature explained the most variation in CO_2 emissions (Fig. 2a, Table 2). Our results indicate that CO_2 emissions are mainly controlled by soil temperature in upland soils, but in seasonally flooded soils, water saturation and the associated low redox potentials become the primary control.

Our results further indicate that CO_2 fluxes were strongly regulated by water saturation and associated redox conditions, but only at temperatures sufficient for microbial activity (Fig. 1, Table 2). Soil redox potentials in the lowland position were typically less than 100 mV during the growing season, but were greater than 400 mV during a majority of the non-growing season (October through January) (Fig. 1d, Table S2). The difference in E_h between the growing and non-growing season in the lowland position indicates that E_h is largely driven by the effects of temperature on microbial consumption of oxygen. We found significantly lower cumulative CO_2 emissions in the lowland position; although this decline in CO_2 production occurred almost entirely during the growing season (Table 1). In the growing season the lowland positions showed a 40 % reduction in CO_2 emissions, yet in the non-growing season the lowland and upland positions had near equal emissions (Table 1; Fig. 1a). These seasonal results indicate that although these seasonally flooded soils become oxygenated, the aerobic period occurs when low seasonal temperatures inhibit microbial activity. In other words, when these seasonally flooded soils experience drained periods with increased oxygen availability, aerobic respiration still remains limited due to low temperatures.

4.2 Relationships between C content and roots, mineralogy and redox

In good agreement with lower decomposition rates in flooded soils (Day and Megonigal 1993; Battle and Golladay 2001) C concentrations were nearly four-times greater than in the upland soil (Table 3). The proximity of our three positions meant that aboveground inputs from litter fall were equal across the transect. However belowground inputs differed significantly; root biomass was substantially lower in the lowland compared to the upland position (p-value < 0.001, ANOVA). Hence, greater C concentrations in the topsoil of the lowland position are likely due to slower rates of decomposition (Day and Megonigal, 1993, Silver et al., 1999, Hall and Silver 2015, Keiluweit et al., 2016) rather than greater above or belowground inputs.

C accumulation in upland soil is often primarily attributed to mineral protection (Kleber et al., 2015; Rasmussen et al., 2018), but it is increasingly acknowledged that oxygen limitations affect C accumulation not only in lowland but also in upland soils (Keiluweit et al., 2017). Similar to a study in tropical forests (Hall and Silver, 2015), we found that C in the surface horizons of upland to wetland transitions increased with lower redox potentials (i.e. oxygen availability) ($r = 0.48$, $p < 0.05$). However, this relationship did not hold true in the subsoils where lower E_h values coincided with lower C concentrations).

C in the topsoil of the lowland position was significantly lower than in the upland position (Table 3). The decrease in C across the transect coincided with a decrease in root biomass, suggesting that a lack of roots is responsible for lower C concentrations in seasonally flooded subsurface horizons. Roots are the primary contributors to C inputs belowground, especially in the subsoil (Rasse et al., 2005; Rumple and Kögel-Knabner,

2011; Hu et al., 2015). However, in our seasonally flooded soils root growth may be restricted by oxygen limitations (Tokarz and Urban, 2015) (Table 3). Therefore, the low C content in the subsoil of the lowland position may be a reflection of restricted root C inputs. Furthermore, we found an overall loss of reactive mineral phases in the lowland subsoils compared to the upland position. Redox-active metals in wetlands can be lost due to reductive dissolution and translocation (Reddy and DeLaune, 2008; Wang et al., 2018), resulting in Fe oxide depletion compared to upland soils. The strong relationship between C and Al_o in the lowland ($r = 0.84$, $p < 0.001$; Table 4) suggests that C content in reducing conditions is largely dependent upon Al oxides for mineral-organic associations, rather than Fe oxides. Taken together, these results indicate that upland, well-drained, soils have a far greater capacity for mineral-protection than poorly-drained soils.

In sum, the seasonally flooded soils in our study had sufficiently long periods of water saturation for C to accumulate in topsoils. C accumulated in the lowland surface soils in spite of lower root C inputs and metal oxide concentrations available for mineral-organic associations. These results suggest that the controlling factor for C accrual in lowland topsoil is water saturation and associated low redox potentials. However, the subsoils in seasonally flooded lowlands had much lower C concentrations than in the upland subsoils, likely due to limited direct C inputs belowground.

4.3 Factors controlling OM composition

To determine C oxidation state and composition along upland-to-lowland transects, we analyzed bulk samples by C NEXAFS and water-extracts by FTICRMS. While NEXAFS analyses of bulk analyses were expected to offer insights into broader changes

in OM composition, high-resolution mass spectrometry analysis of water extracts was conducted to target bioavailable compounds small enough to be used in microbial respiration. We hypothesized that thermodynamic constraints during anaerobic periods would inhibit the microbial respiration of chemically-reduced organic compounds in the lowland positions of seasonal wetlands (Keiluweit et al., 2016). Conversely, we expected the upland positions to contain more oxidized organic C compounds as a result of increased oxygen availability for microbial respiration. Analysis of the C chemistry of the bulk soil and water extractable C supported our predictions of a greater abundance of chemically reduced compounds in the lowland positions, but only in the topsoil (Fig. 4 and 5). Along the upland-to-lowland transects, bulk surface soil C showed an increase in relatively reduced aliphatic and aromatic functional groups, paralleled by a decrease in carboxylic groups. Both the increase in relatively reduced aliphatic functional groups and decrease in relatively oxidized carboxylic was significantly correlated with E_h across the transect. Similarly, NOSC of water extractable organic compounds in the surface horizons decreased from upland to lowland positions (Fig 5b), which is indicative of a greater abundance of chemically reduced compounds. The average molecular weight of the water extractable C in the surface soils was nearly 20% greater in the lowland than the upland position (Fig. 5c). While the average molecular weight of the water extractable C in the seasonally flooded soil was slightly larger than the upland soil, the average molecular weight is sufficiently small (average MW = 100-250 Da) to be assimilated and processes in microbial respiration. That suggests that thermodynamic constraints on microbial respiration (Keiluweit et al. 2016; Boye et al., 2017) rather than kinetic limitations on

oxidative polymerization, are primarily responsible for the accumulation of chemically reduced organic compounds under anaerobic conditions.

Contrary to our expectation, the subsoil showed the reverse trend – where C become chemically more oxidized along the upland-to-lowland transect (Fig. 4 and 5). Lowland subsoils showed a greater abundance of carboxylic C and a lower abundance in aromatic and aliphatic C than upland subsoils (Fig. 4a). Unlike the topsoil horizons, NOSC values increased (Fig. 5b) along the transects in the subsurface horizons, indicative of the presence of more chemically-oxidized C in the lowland subsoils. This unexpected result may point to other factors besides low redox potential that influence C chemistry. The dramatic difference in subsoil root biomass between upland and lowland soils suggest that these changes may largely be driven by root biomass.

Subsoil C stocks are largely derived from root inputs (Ota et al., 2013; Rasse at al., 2005), which are composed of chemically reduced aliphatic (e.g. suberin and cutin) and aromatic compounds (e.g. lignin and tannins) (Mueller et al., 2013; Spielvogel et al., 2014). Such root-derived inputs may have resulted in greater contributions of chemically-reduced compounds to upland subsoil (Liang and Balser, 2008). In contrast, the lowland subsoils were nearly void of roots and had low C concentrations. Together, this suggests that the C in the subsoil does not originate from roots but rather as dissolved organic C (DOC) leached downward from the topsoil. Wetland subsoils typically have higher concentrations of DOC compared to upland forest soils (Kalbitz et al., 2000; Fiedler and Kalbitz, 2003). In reduced soils, the limited mineral organic associations with redox-active metals permits higher concentrations of DOC to be transported down the soil (Kaiser and Guggenberger, 2000).

Together these results suggest that subsoil C in seasonally flooded soil soluble, plant-derived C that is leached down the soil profile during water table drawdown.

CHAPTER 5

IMPLICATIONS

Our results indicate that oxygen limitations due to water saturation is the predominate control on C storage in freshwater mineral wetlands. Warmer temperatures and less rain in the summer months is predicted to alter the duration and timing of flooding in wetlands throughout the Northeastern US (Fan et al., 2015; Brooks, 2009). Consequently, wetland soils will become more oxygenated, lifting the redox controls on C decomposition and promoting more rapid aerobic respiration and greater CO_2 emissions. Our results show that seasonal timing of anaerobic periods is critically important to C accumulation within wetlands, as temperature ultimately controls the microbial decomposition of the C stored therein. Theoretically, if lowland soils remain anaerobic during a significant portion of the growing season, with aerobic periods occurring in the non-growing season, microbial decomposition rates should be sufficiently low for C to accumulate. Additionally, prolonged water saturation results in a loss of reactive metals which leads to a diminished capacity for mineral protection in these ecosystems. Thus C stored in wetlands would be readily accessible for microbial decomposition and respiration upon drainage. The general lack of mineral protection in freshwater mineral wetlands magnifies the importance of anaerobic control on C storage in these vulnerable ecosystems.

C pools in wetlands may also be impacted by encroachment of upland plants into previously flooded lowland territory. Recent studies suggest that colonization by deep-rooting upland plants will offset some of the C loss upon drainage of former wetlands through additional C inputs (Gorham et al., 1991; Trettin et al., 2006). However, the lack

of reactive metal phases observed in seasonally flooded soils investigated here suggests a low capacity for mineral-organic associations and, consequently, a low potential for long term storage of additional root inputs.

CHAPTER 6

CONCLUSIONS

Our results show that periodic flooding is the primary control on CO_2 emissions, C concentrations, and OM composition in seasonally flooded lowland soils. Importantly, we see distinctly different mechanisms controlling C concentration and composition in surface versus subsurface soils, which sharply contrasts those governing the upland system. In spite of seasonal re-oxygenation of the surface soil, periodic flooding and the associated oxygen limitations, imposed sufficient metabolic constraints on microbial respiration to cause the accumulation of large amounts of aboveground litter-derived, chemically reduced C compounds in the soil surface. In the subsurface, however, water table fluctuations restricted root growth and removed reducible Fe oxides. This observation suggests that the lack of root C inputs and mineral protection are primarily responsible for the low subsurface C accumulation. C accumulating at depth was relatively oxidized and predominantly plant-derived, suggesting that water table fluctuations promote the leaching of litter-derived DOC from the surface to deeper soils. Our findings indicate that C accrual in seasonal wetlands is due primarily to oxygen limitations in the surface soil, and that the overall deficiency of mineral protection leaves these C stocks highly vulnerable to climate change.

Table 1 Cumulative CO_2 emissions (+/- standard error) for each landscape position

Position	Cumulative mole CO_2 m^{-2} Total	Cumulative mole CO_2 m^{-2} Growing season	Cumulative mole CO_2 m^{-2} Non-growing season	Cumulative mole CO_2 m^{-2} C^{-1}
Upland	54^{a} (1.1)	38^{a} (1.6)	16^{a} (0.8)	1.15^{b} (0.23)
Transition	53^{a} (0.9)	33^{a} (1.5)	20^{a} (0.9)	1.03^{a} (0.22)
Lowland	39^{a} (0.8)	24^{a} (1.3)	15^{a} (0.7)	0.39^{a} (0.11)

Letter designations are Tukey's post hoc honesty test results. Different letter designations indicate a p-value of < 0.05.

Table 2 Regression analysis (r) results of potential environmental variables that predict CO_2 emissions along a moisture gradient

Environmental Variable	Season	Upland	Transition	Lowland
Soil temperature[#]	Full	0.72***	0.60***	0.53***
	GS	0.62***	0.56***	0.45***
	NGS	0.79***	0.81***	0.69***
Water Table Depth[S]	Full	-0.03	-0.05	-0.30**
	GS	-0.32**	-0.14	-0.55***
	NGS	-0.20	-0.17	-0.35**
Volumetric Moisture Content[S]	Full	0.20*	-0.44***	-0.32***
	GS	0.10	-0.72***	-0.51***
	NGS	-0.10	-0.37**	-0.37**
Soil Redox Potential[S]	Full	0.10	0.10	0.01
	GS	0.05	0.41***	0.40***
	NGS	0.06	0.08	0.27*

Full = entire year, GS = growing season, NGS = non-growing season.

[#] Arrhenius fit

[s] Linear fit

Significance codes: < 0.001 = '***', 0.01 = '**', 0.05 =' *'

Table 3 Mean (+/- standard error) soil properties of each landscape position and horizon

Horizon	Total Carbon (%)	C:N	Root Biomass (mg g^{-1} soil)	pH	Silt + Clay (%)	Fe_o (mg g^{-1} soil)	Al_o (mg g^{-1} soil)
Upland							
A	2.3^{ab} (0.5)	11^{a} (2.5)	61^{b} (27)	4.98 (0.2)	48^{a} (11)	3.6^{b} (0.5)	5.1^{c} (0.8)
B	1.1^{ab} (0.3)	13^{a} (3.4)	14^{ab} (3)	5.22^{a} (0.2)	39^{a} (11)	2.4^{ab} (0.7)	5.7^{c} (1.9)
C	0.64^{a} (0.1)	13^{a} (5.3)	6^{a} (3)	5.29^{a} (0.1)	37^{a} (12)	1.7^{ab} (0.4)	3.6^{abc} (0.8)
Transition							
A	3.9^{bc} (1.5)	14^{a} (1.6)	48^{b} (17)	4.97^{a} (0.2)	51^{a} (10)	1.2^{a} (0.4)	2.5^{abc} (0.3)
B/C	0.64^{a} (0.1)	6.4^{a} (1.4)	15^{ab} (6)	5.38^{a} (0.1)	41^{a} (11)	1.5^{ab} (0.3)	1.9^{abc} (0.3)
Cg	0.36^{a} (0.1)	5.0^{a} (3.8)	3^{a} (1)	5.43^{a} (0.2)	59^{a} (10)	1.3^{ab} (0.3)	1.3^{ab} (0.4)
Lowland							
A	8.2^{c} (2.4)	16^{a} (1.1)	6^{a} (2)	4.98^{a} (0.1)	50^{a} (13)	1.5^{ab} (0.4)	4.1^{bc} (1.1)
C	1.9^{ab} (0.5)	13^{a} (3.7)	2^{a} (0.6)	5.29^{a} (0.1)	66^{a} (9)	1.0^{a} (0.3)	2.6^{abc} (0.5)
Cg	0.36^{a} (0.02)	7.3^{a} (4.9)	0.7^{a} (0.5)	5.37^{a} (0.1)	70^{a} (9)	2.9^{ab} (0.7)	1.0^{a} (0.2)

Table 4 Linear regression (r) values for potential environmental variables that predict total carbon concentrations for each landscape position

Environmental Variable	Upland	Transition	Lowland
Silt + Clay	0.10	0.22	0.10
Fe_o	0.70***	0.03	-0.14
Al_o	0.50*	0.10	0.84***
Root biomass	0.59**	0.72***	0.66**
Redox potential	0.32	0.10	0.14

Significance codes: < 0.001 = '***', 0.01 = '**', 0.05 =' *'

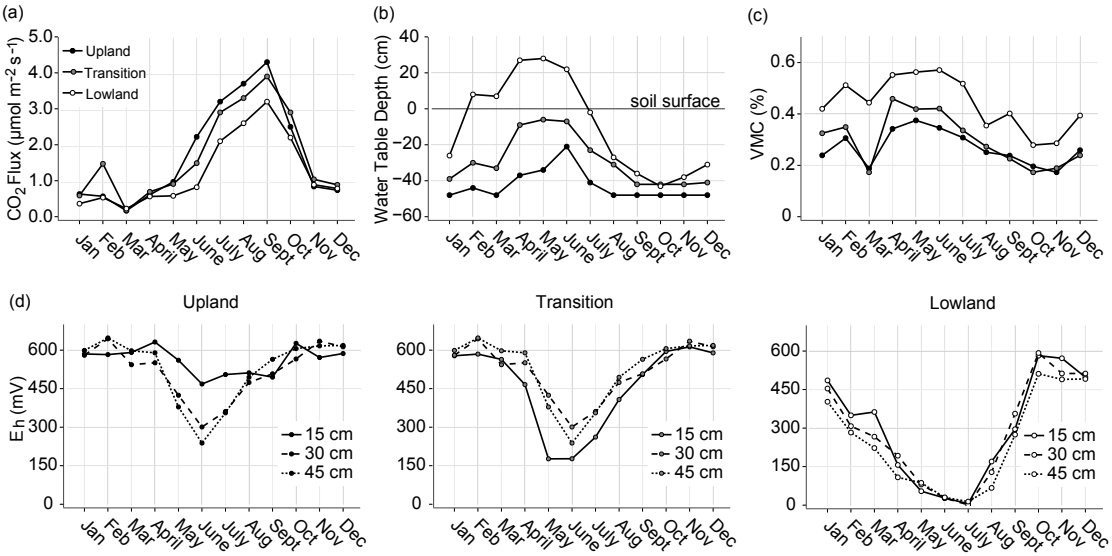

Figure 1 Seasonal dynamics of soil respiration, water table depth, volumetric moisture content, and redox potentials among three landscape positions along a moisture gradient. (a) Mean monthly soil respiration fluxes (CO_2 μmol m^{-2} s^{-1}), (b) mean monthly water table depths (cm), (c) mean monthly volumetric moisture contents (%) for the three landscape positions; summit, rim, basin, (d) mean monthly soil redox potentials (mV) for the three landscape positions and at three depths within each landscape position; 15, 30, and 45 cm. Redox potentials are standardized from a calomel to a hydrogen electrode. Values are means from six replicate transects.

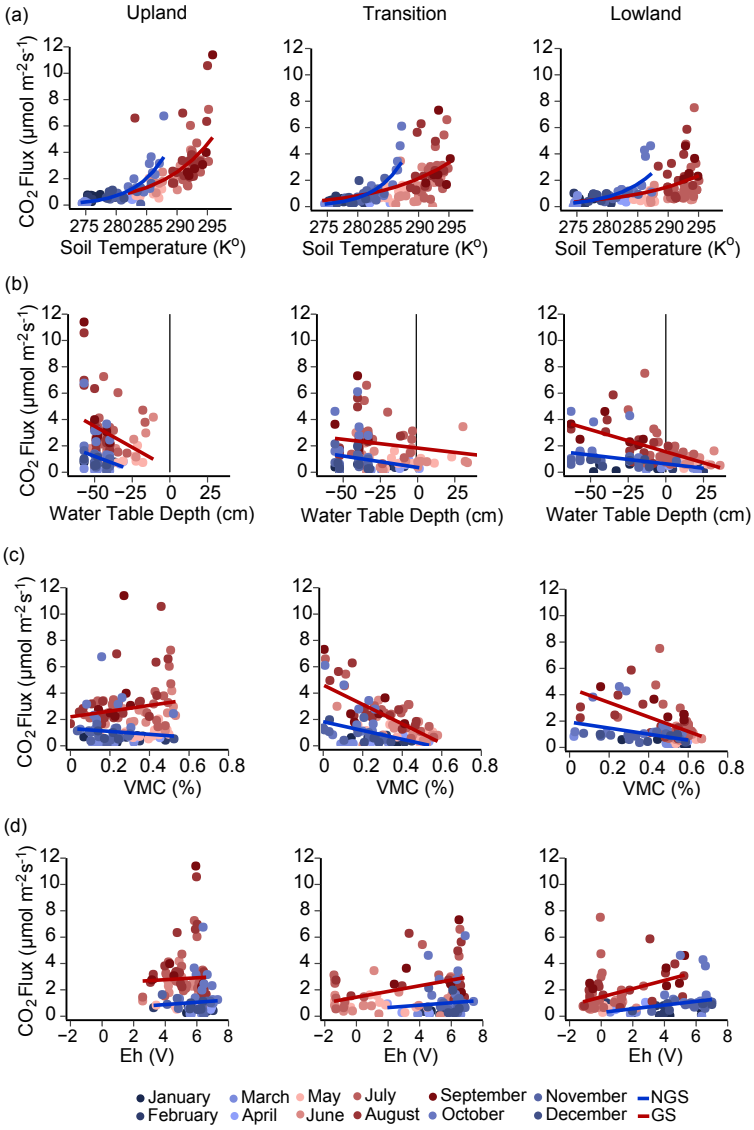

Figure 4 Regression analyses between pairwise comparisons of soil temperature, water table depth, moisture content, and redox potential with soil respiration. (a) Annual soil temperature (°K) at 10 cm depth plotted against carbon dioxide emission rates (µmol m^{-2} s^{-1}) for each landscape position with Arrhenius regressions for growing (May-September; red-scale markers) and non-growing season (October-April; blue-scale markers). (b) Annual water table depths (cm) plotted against carbon dioxide emission rates (µmol m^{-2} s^{-1}) for the three landscape positions. Water table depths less than zero are below soil surface; depths greater than zero are above soil surface. Linear regressions plotted for growing and non-growing season. (c) Annual volumetric moisture contents (%) at 10 cm depth plotted against carbon dioxide emission rates (µmol m^{-2} s^{-1}) for the three landscape positions. Linear regressions plotted for growing and non-growing season. (d) Annual soil redox potentials (mV) at 15 cm depth plotted against carbon dioxide emission rates (µmol m^{-2} s^{-1}) for the three landscape positions. Linear regressions plotted for growing and non-growing season.

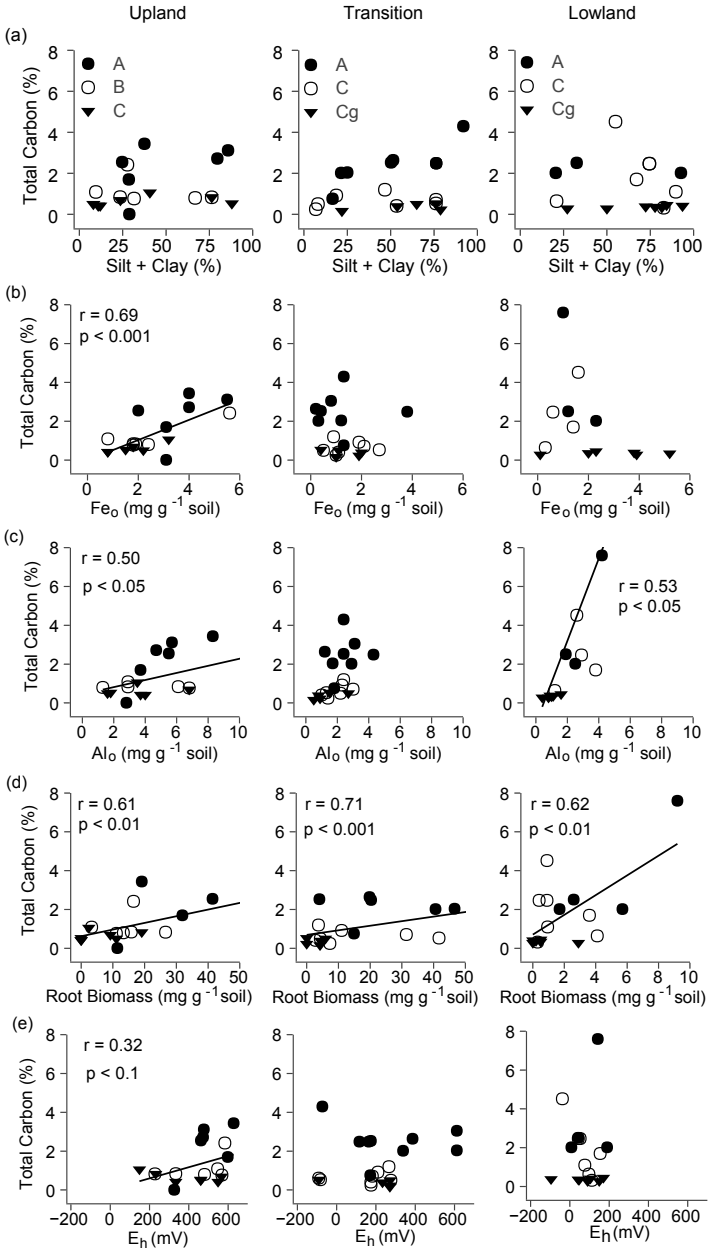

Figure 10 Pairwise relationships between total C concentrations and soil biogeochemical variables. Total C concentrations plotted against (a) silt plus clay (%), (b) ammonium oxalate extractable Fe (Fe_o; mg g^{-1} soil), (c) Al (Al_o; mg g^{-1} soil), (d) root biomass (mg g^{-1} soil), and (e) mean E_h during the growing season standardized to a hydrogen reference electrode (mV). Significant linear regressions are plotted for each landscape position.

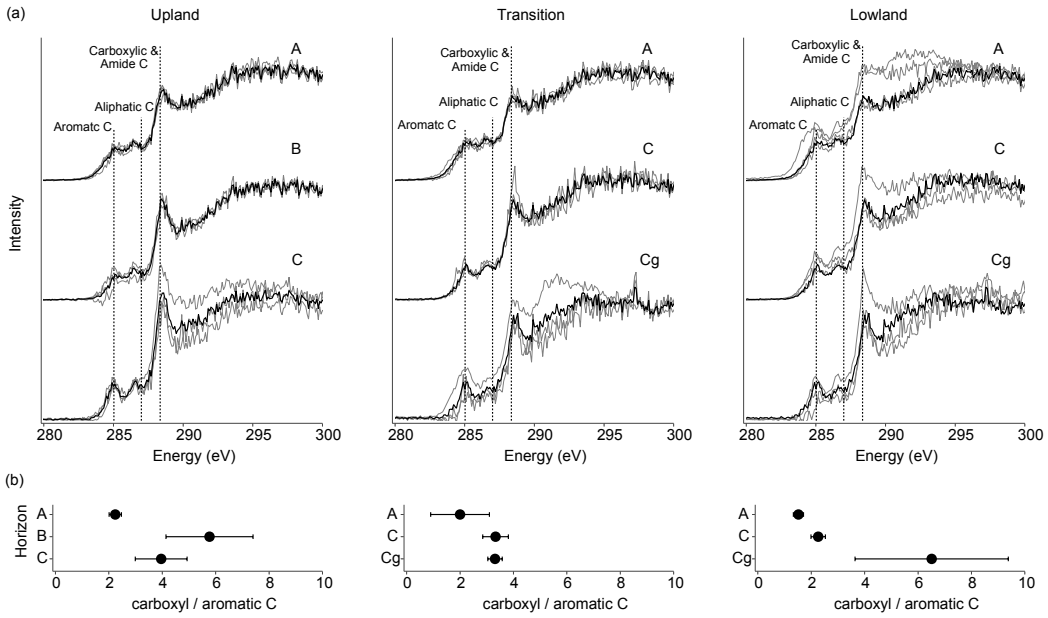

Figure 13 Individual and mean C (1s) NEXAFS spectra for each landscape position and horizon. (a) Individual NEXAFS spectra for each replicate sample (grey) with the resulting average (black). Peaks of particular interest for aromatic C (285.03 eV), aliphatic C (287.2 eV), and carboxylic (288.35 eV) are denoted by dotted vertical lines. (b) Mean carboxyl to aromatic C ratios plotted for each landscape position and depth; error bars are standard error.

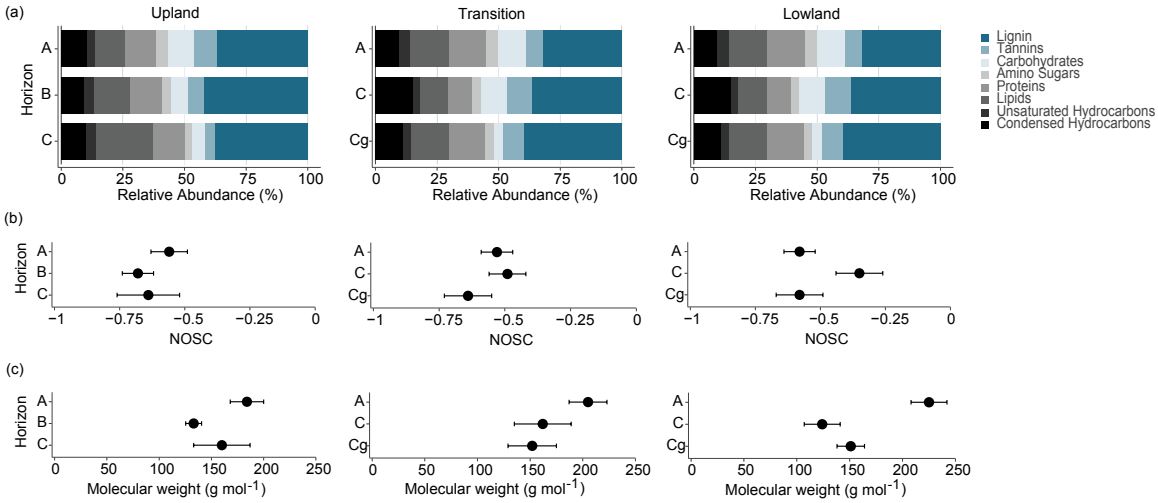

Figure 18 FT-ICR-MS relative abundances of C compound classes, average NOSC and molecular weights. (a) Relative abundances of compound classes in water extractable OM calculated using Van Krevelen plots based on O/C and H/C ratios (Tfaily et al. 2015). Grey-scale colors denoted primarily plant-derived compounds while blue-scale compounds denote microbial-derived OM compounds. Mean (b) NOSC and molecular weight (g mol^{-1}) values of water extractable OM determined by FT-ICR-MS for each landscape position and horizon. Error bars are standard error.

BIBLIOGRAPHY

ASRIS, ASRIS: Australian Soil Resource Information System., http://www.asris.csiro.au. Accessed September, 2016.

Battle, J. M. and Golladay, S. W.: Hydroperiod Influence on Breakdown of Leaf Litter in Cypress-gum Wetlands, The American Midland Naturalist, 146(1), 128–145, doi:10.1674/0003-0031(2001)146[0128:HIOBOL]2.0.CO;2, 2001.

Bouma, J.: Hydrology and Soil Genesis of Soils with Aquic Moisture Regimes, in Developments in Soil Science, vol. 11, pp. 253–281, Elsevier., 1983.

Boye, K., Noël, V., Tfaily, M. M., Bone, S. E., Williams, K. H., Bargar, J. R. and Fendorf, S.: Thermodynamically controlled preservation of organic carbon in floodplains, Nature Geoscience, 10(6), 415–419, doi:10.1038/ngeo2940, 2017.

Bradford, M. A., Keiser, A. D., Davies, C. A., Mersmann, C. A. and Strickland, M. S.: Empirical evidence that soil carbon formation from plant inputs is positively related to microbial growth, Biogeochemistry, 113(1–3), 271–281, doi:10.1007/s10533-012-9822-0, 2013.

Bridgham, S. D., Patrick Megonigal, J., Keller, J. K., Bliss, N. B. and Trettin, C.: The carbon balance of North American wetlands, Wetlands, 26(4), 889–916, 2006.

Brooks, R. T.: A review of lowland morphology and pool hydrology of isolated ponded wetlands: implications for seasonal forest pools of the northeastern United States, Wetlands ecology and management, 13(3), 335–348, 2005.

Chen, H., Zou, J., Cui, J., Nie, M. and Fang, C.: Wetland drying increases the temperature sensitivity of soil respiration, Soil Biology and Biochemistry, 120, 24–27, doi:10.1016/j.soilbio.2018.01.035, 2018.

Chmura, G. L., Anisfeld, S. C., Cahoon, D. R. and Lynch, J. C.: Global carbon sequestration in tidal, saline wetland soils, Global Biogeochemical Cycles, 17(4), n/a-n/a, doi:10.1029/2002GB001917, 2003.

D'Amore, D. V., Stewart, S. R. and Huddleston, J. H.: Saturation, Reduction, and the Formation of Iron–Manganese Concretions in the Jackson-Frazier Wetland, Oregon, Soil Science Society of America Journal, 68(3), 1012, doi:10.2136/sssaj2004.1012, 2004.

DARKE, A. K. and WALBRIDGE, M. R.: Al and Fe Biogeochemistry in a floodplain forest: Implications for P retention, , 32, n.d.

Davidson, E. A., Samanta, S., Caramori, S. S. and Savage, K.: The Dual Arrhenius and Michaelis-Menten kinetics model for decomposition of soil organic matter at hourly to seasonal time scales, Global Change Biology, 18(1), 371–384, doi:10.1111/j.1365-2486.2011.02546.x, 2012.

Day, F. P. and Megonigal, J. P.: The relationship between variable hydroperiod, production allocation, and belowground organic turnover in forested wetlands, Wetlands, 13(2), 115–121, doi:10.1007/BF03160871, 1993.

Erwin, K. L.: Wetlands and global climate change: the role of wetland restoration in a changing world, Wetlands Ecology and Management, 17(1), 71–84, doi:10.1007/s11273-008-9119-1, 2009.

Fan, F., Bradley, R. S. and Rawlins, M. A.: Climate change in the Northeast United States: An analysis of the NARCCAP multimodel simulations: NORTHEAST U.S. CLIMATE CHANGE, Journal of Geophysical Research: Atmospheres, 120(20), 10,569-10,592, doi:10.1002/2015JD023073, 2015.

Fenner, N. and Freeman, C.: Drought-induced carbon loss in peatlands, Nature Geoscience, 4(12), 895–900, doi:10.1038/ngeo1323, 2011.

Fiedler, S., Vepraskas, M. J. and Richardson, J. L.: Soil Redox Potential: Importance, Field Measurements, and Observations, in Advances in Agronomy, vol. 94, pp. 1–54, Elsevier., 2007.

Fissore, C., Giardina, C. P., Kolka, R. K. and Trettin, C. C.: Soil organic carbon quality in forested mineral wetlands at different mean annual temperature, Soil Biology and Biochemistry, 41(3), 458–466, doi:10.1016/j.soilbio.2008.11.004, 2009.

Freeman, C., Ostle, N., and Kang, H. (2001) An enzymic “latch” on a global carbon store. Nature 409:149.

Gorham, E.: Northern Peatlands: Role in the Carbon Cycle and Probable Responses to Climatic Warming, Ecological Applications, 1(2), 182–195, doi:10.2307/1941811, 1991.

Hall, S. J. and Silver, W. L.: Reducing conditions, reactive metals, and their interactions can explain spatial patterns of surface soil carbon in a humid tropical forest, Biogeochemistry, 125(2), 149–165, doi:10.1007/s10533-015-0120-5, 2015.

Hall, S. J., McDowell, W. H. and Silver, W. L.: When Wet Gets Wetter: Decoupling of Moisture, Redox Biogeochemistry, and Greenhouse Gas Fluxes in a Humid Tropical Forest Soil, Ecosystems, 16(4), 576–589, doi:10.1007/s10021-012-9631-2, 2013.

Hall, S. J., Treffkorn, J. and Silver, W. L.: Breaking the enzymatic latch: impacts of reducing conditions on hydrolytic enzyme activity in tropical forest soils, Ecology, 95(10), 2964–2973, doi:10.1890/13-2151.1, 2014.

Havens, K. J.: The effect of vegetation on soil redox within a seasonally flooded forested system, Wetlands, 17(2), 237–242, 1997.

Hedges, J. I. and Stern, J. H.: Carbon and nitrogen determinations of carbonate-containing solids, Limnology and Oceanography, 29(3), 657–663, doi:10.4319/lo.1984.29.3.0657, 1984.

Hu, Q., Cai, J., Yao, B., Wu, Q., Wang, Y. and Xu, X.: Plant-mediated methane and nitrous oxide fluxes from a carex meadow in Poyang Lake during drawdown periods, Plant and Soil, 400(1–2), 367–380, doi:10.1007/s11104-015-2733-9, 2016.

Ise, T., Dunn, A. L., Wofsy, S. C. and Moorcroft, P. R.: High sensitivity of peat decomposition to climate change through water-table feedback, Nature Geoscience, 1(11), 763–766, doi:10.1038/ngeo331, 2008.

J. C. Munch and J. C. G. Ottow: Reductive Transformation Mechanism of Ferric Oxides in Hydromorphic Soils, Ecological Bulletins, (35,), 383–394, 1983.

Jones, D. L., Nguyen, C. and Finlay, R. D.: Carbon flow in the rhizosphere: carbon trading at the soil–root interface, Plant and Soil, 321(1–2), 5–33, doi:10.1007/s11104-009-9925-0, 2009.

Kaiser, K. and Guggenberger, G.: The role of DOM sorption to mineral surfaces in the preservation of organic matter in soils, Organic Geochemistry, 31(7–8), 711–725, doi:10.1016/S0146-6380(00)00046-2, 2000.

Kallenbach, C. M., Frey, S. D. and Grandy, A. S.: Direct evidence for microbial-derived soil organic matter formation and its ecophysiological controls, Nature Communications, 7, 13630, doi:10.1038/ncomms13630, 2016.

Keiluweit, M., Nico, P. S., Kleber, M. and Fendorf, S.: Are oxygen limitations under recognized regulators of organic carbon turnover in upland soils?, Biogeochemistry, 127(2–3), 157–171, doi:10.1007/s10533-015-0180-6, 2016.

Keiluweit, M., Wanzek, T., Kleber, M., Nico, P. and Fendorf, S.: Anaerobic microsites have an unaccounted role in soil carbon stabilization, Nature Communications, 8(1), doi:10.1038/s41467-017-01406-6, 2017.

Kim, S., Kramer, R. W. and Hatcher, P. G.: Graphical Method for Analysis of Ultrahigh-Resolution Broadband Mass Spectra of Natural Organic Matter, the Van Krevelen Diagram, Analytical Chemistry, 75(20), 5336–5344, doi:10.1021/ac034415p, 2003.

Kirwan, M. L. and Blum, L. K.: Enhanced decomposition offsets enhanced productivity and soil carbon accumulation in coastal wetlands responding to climate change, Biogeosciences, 8(4), 987–993, doi:10.5194/bg-8-987-2011, 2011.

Kleber, M., Eusterhues, K., Keiluweit, M., Mikutta, C., Mikutta, R. and Nico, P. S.: Mineral–Organic Associations: Formation, Properties, and Relevance in Soil Environments, in Advances in Agronomy, vol. 130, pp. 1–140, Elsevier., 2015.

Kögel-Knabner, I.: The macromolecular organic composition of plant and microbial residues as inputs to soil organic matter, Soil Biology and Biochemistry, 34(2), 139–162, doi:10.1016/S0038-0717(01)00158-4, 2002.

Koh, H.-S., Ochs, C. A. and Yu, K.: Hydrologic gradient and vegetation controls on CH4 and CO2 fluxes in a spring-fed forested wetland, Hydrobiologia, 630(1), 271–286, doi:10.1007/s10750-009-9821-x, 2009.

Krauss, K. W. and Whitbeck, J. L.: Soil Greenhouse Gas Fluxes during Wetland Forest Retreat along the Lower Savannah River, Georgia (USA), Wetlands, 32(1), 73–81, doi:10.1007/s13157-011-0246-8, 2012.

Laine, J., Silvola, J., Tolonen, K., Alm, J., Nykänen, H., Vasander, H., Sallantaus, T., Savolainen, I., Sinisalo, J. and Martikainen, P. J.: Effect of water-level drawdown on global climatic warming: Northern peatlands, Ambio, 179–184, 1996.

Letey, J., and Stolzy, L.H. (1964) Measurement of Oxygen Diffusion Rates with the Platinum Microelectrode. Hilgardia 35: 545-554.

Li, W. and Johnson, C. E.: Relationships among pH, aluminum solubility and aluminum complexation with organic matter in acid forest soils of the Northeastern United States, Geoderma, 271, 234–242, doi:10.1016/j.geoderma.2016.02.030, 2016.

Liang, C. and Balser, T. C.: Preferential sequestration of microbial carbon in subsoils of a glacial-landscape toposequence, Dane County, WI, USA, Geoderma, 148(1), 113–119, doi:10.1016/j.geoderma.2008.09.012, 2008.

Liu, Y., Wan, K., Tao, Y., Li, Z., Zhang, G., Li, S. and Chen, F.: Carbon Dioxide Flux from Rice Paddy Soils in Central China: Effects of Intermittent Flooding and Draining Cycles, edited by D. Q. Fuller, PLoS ONE, 8(2), e56562, doi:10.1371/journal.,pone.0056562, 2013.

Lloyd, J. and Taylor, J. A.: On the Temperature Dependence of Soil Respiration, Functional Ecology, 8(3), 315, doi:10.2307/2389824, 1994.

Loeppert, R. H., Inskeep, W.P.: Methods of Soil Analysis. Part 3. Chemical Methods: Iron. Soil Science Society of America and American Society of Agronomy, Madison, WI, USA, 639-644, 1996.

Logue, J. B., Stedmon, C. A., Kellerman, A. M., Nielsen, N. J., Andersson, A. F., Laudon, H., Lindström, E. S. and Kritzberg, E. S.: Experimental insights into the importance of aquatic bacterial community composition to the degradation of dissolved organic matter, The ISME Journal, 10(3), 533–545, doi:10.1038/ismej.2015.131, 2016.

Madigan, T. M., Martinko, J. M., and Parker, J.: Brock Biology of Microorganisms, Pearson Education, Inc., Upper Saddle, NJ, USA, 1984.

McInerney, E. and Helton, A. M.: The Effects of Soil Moisture and Emergent Herbaceous Vegetation on Carbon Emissions from Constructed Wetlands, Wetlands, 36(2), 275–284, doi:10.1007/s13157-016-0736-9, 2016.

McNicol, G. and Silver, W. L.: Non-linear response of carbon dioxide and methane emissions to oxygen availability in a drained histosol, Biogeochemistry, 123(1–2), 299–306, doi:10.1007/s10533-015-0075-6, 2015.

Mikutta, R., Mikutta, C., Kalbitz, K., Scheel, T., Kaiser, K. and Jahn, R.: Biodegradation of forest floor organic matter bound to minerals via different binding mechanisms, Geochimica et Cosmochimica Acta, 71(10), 2569–2590, doi:10.1016/j.gca.2007.03.002, 2007.

Miltner, A., Kindler, R., Knicker, H., Richnow, H.-H. and Kästner, M.: Fate of microbial biomass-derived amino acids in soil and their contribution to soil organic matter, Organic Geochemistry, 40(9), 978–985, doi:10.1016/j.orggeochem.2009.06.008, 2009.

Mitsch, W. J., Bernal, B., Nahlik, A. M., Mander, Ü., Zhang, L., Anderson, C. J., Jørgensen, S. E. and Brix, H.: Wetlands, carbon, and climate change, Landscape Ecology, 28(4), 583–597, doi:10.1007/s10980-012-9758-8, 2013.

Moore, T. R. and Knowles, R.: THE INFLUENCE OF WATER TABLE LEVELS ON METHANE AND CARBON DIOXIDE EMISSIONS FROM PEATLAND SOILS, Canadian Journal of Soil Science, 69(1), 33–38, doi:10.4141/cjss89-004, 1989.

Moore, T. R., Roulet, N. T., and Waddington, J. M.: Uncertainty in Predicting the Effect of Climatic Change on the Carbon Cycling of Canadian Peatlands, Climatic Change, 40(1), 229-245, 1998.

Mueller, P., Jensen, K. and Megonigal, J. P.: Plants mediate soil organic matter decomposition in response to sea level rise, Global Change Biology, 22(1), 404–414, doi:10.1111/gcb.13082, 2016.

National Centers for Environmental Information, National Oceanic and Atmospheric Administration, https://www.ncei.noaa.gov, last access: May 2018.

Neckles, H. A. and Neill, C. Hydrologic controls of litter decomposition in seasonally flooded prairie marshes, Hydrobiologia 286: 155, doi:10.1007/BF00006247, 1994.

Ota, M., Nagai, H. and Koarashi, J.: Root and dissolved organic carbon controls on subsurface soil carbon dynamics: A model approach: CONTROLS ON SUBSURFACE CARBON DYNAMICS, Journal of Geophysical Research: Biogeosciences, 118(4), 1646–1659, doi:10.1002/2013JG002379, 2013.

Patrick, W. H. and Delaune, R. D.: Characterization of the Oxidized and Reduced Zones in Flooded Soil, Soil Science Society of America Journal, 36(4), 573, doi:10.2136/sssaj1972.03615995003600040024x, 1972.

Paul, E. A.: The nature and dynamics of soil organic matter: Plant inputs, microbial transformations, and organic matter stabilization, Soil Biology and Biochemistry, 98, 109–126, doi:10.1016/j.soilbio.2016.04.001, 2016.

Pezeshki, S. R. and DeLaune, R. D.: Soil Oxidation-Reduction in Wetlands and Its Impact on Plant Functioning, Biology, 1(3), 196–221, doi:10.3390/biology1020196, 2012.

Phillips, S. C., Varner, R. K., Frolking, S., Munger, J. W., Bubier, J. L., Wofsy, S. C. and Crill, P. M.: Interannual, seasonal, and diel variation in soil respiration relative to ecosystem respiration at a wetland to upland slope at Harvard Forest: SOIL RESPIRATION AT HARVARD FOREST, Journal of Geophysical Research: Biogeosciences, 115(G2), n/a-n/a, doi:10.1029/2008JG000858, 2010.

Porras, R. C., Hicks Pries, C. E., McFarlane, K. J., Hanson, P. J. and Torn, M. S.: Association with pedogenic iron and aluminum: effects on soil organic carbon storage and stability in four temperate forest soils, Biogeochemistry, 133(3), 333–345, doi:10.1007/s10533-017-0337-6, 2017.

Rasmussen, C., Southard, R. J. and Horwath, W. R.: Mineral control of organic carbon mineralization in a range of temperate conifer forest soils, Global Change Biology, 12(5), 834–847, doi:10.1111/j.1365-2486.2006.01132.x, 2006.

Rasmussen, C., Heckman, K., Wieder, W. R., Keiluweit, M., Lawrence, C. R., Berhe, A. A., Blankinship, J. C., Crow, S. E., Druhan, J. L., Hicks Pries, C. E., Marin-Spiotta, E., Plante, A. F., Schädel, C., Schimel, J. P., Sierra, C. A., Thompson, A. and Wagai, R.: Beyond clay: towards an improved set of variables for predicting soil organic matter content, Biogeochemistry, 137(3), 297–306, doi:10.1007/s10533-018-0424-3, 2018.

Rasse, D. P., Rumpel, C. and Dignac, M.-F.: Is soil carbon mostly root carbon? Mechanisms for a specific stabilisation, Plant and Soil, 269(1–2), 341–356, doi:10.1007/s11104-004-0907-y, 2005.

Reddy, K. R., and DeLaune, R. D.: Biogeochemistry of Wetlands: Science and Applications, CRC Press, Boca Raton, FL, USA, 2008.

Regiern, T. et al.: Performance and capabilities of the Canadian dragon: the SGM beamline at the Canadian Light Source, Nucl. Instrum. Methods Phys. Res. A, 582, 93-95, 2007.

Rumpel, C. and Kögel-Knabner, I.: Deep soil organic matter—a key but poorly understood component of terrestrial C cycle, Plant and Soil, 338(1–2), 143–158, doi:10.1007/s11104-010-0391-5, 2011.

Rumpel, C., Kögel-Knabner, I. and Bruhn, F.: Vertical distribution, age, and chemical composition of organic carbon in two forest soils of different pedogenesis, Organic Geochemistry, 33(10), 1131–1142, doi:10.1016/S0146-6380(02)00088-8, 2002.

RStudio Team (2016). RStudio: Integrated Development for R. RStudio, Inc., Boston, MA. URL http://www.rstudio.com/.

Saidy, A. R., Smernik, R. J., Baldock, J. A., Kaiser, K., Sanderman, J. and Macdonald, L. M.: Effects of clay mineralogy and hydrous iron oxides on labile organic carbon stabilisation, Geoderma, 173–174, 104–110, doi:10.1016/j.geoderma.2011.12.030, 2012.

Saidy, A. R., Smernik, R. J., Baldock, J. A., Kaiser, K. and Sanderman, J.: The sorption of organic carbon onto differing clay minerals in the presence and absence of hydrous iron oxide, Geoderma, 209–210, 15–21, doi:10.1016/j.geoderma.2013.05.026, 2013.

Schumacher, M., Christl, I., Vogt, R. D., Bartmettler, K., Jacobsen, C., and Kretzschmar, R.: Chemical composition of aquatic dissolved organic matter in five boreal forest catchments samples in spring and fall seasons, Biogeochemistry, (80)3, 263-275, doi: 10.1007/s10533-006-9022-x, 2006.

Sierra, C. A.: Temperature sensitivity of organic matter decomposition in the Arrhenius equation: some theoretical considerations, Biogeochemistry, 108(1–3), 1–15, doi:10.1007/s10533-011-9596-9, 2012.

Silver, W. L., Lugo, A. E. and Keller, M.: Soil oxygen availability and biogeochemistry along rainfall and topographic gradients in upland wet tropical forest soils, Biogeochemistry, 44(3), 301–328, doi:10.1007/BF00996995, 1999.

Silvola, J., Alm, J., Ahlholm, U., Nykanen, H. and Martikainen, P. J.: CO 2 Fluxes from Peat in Boreal Mires under Varying Temperature and Moisture Conditions, The Journal of Ecology, 84(2), 219, doi:10.2307/2261357, 1996.

Soil Survey Staff. Soil taxonomy: A basic system of soil classification for making and interpreting soil surveys. 2nd edition. Natural Resources Conservation Service. U.S. Department of Agriculture Handbook 436, 1996.

Solomon, D., Lehmann, J., Kinyangi, J., Liang, B., and Schäfer, T.: Carbon K-Edge NEXAFS and FTIR-ATR Spectroscopic Investigation of Organic Carbon Speciation in Soils, Soil Sci. Soc. of America Journal, 69(1), 107, doi: 10.2136/sssaj2005.0107dup, 2005.

Spielvogel, S., Prietzel, J., Leide, J., Riedel, M., Zemke, J. and Kögel-Knabner, I.: Distribution of cutin and suberin biomarkers under forest trees with different root systems, Plant and Soil, 381(1–2), 95–110, doi:10.1007/s11104-014-2103-z, 2014.

Sutton-Grier, A. E., Keller, J. K., Koch, R., Gilmour, C. and Megonigal, J. P.: Electron donors and acceptors influence anaerobic soil organic matter mineralization in tidal marshes, Soil Biology and Biochemistry, 43(7), 1576–1583, doi:10.1016/j.soilbio.2011.04.008, 2011.

Tiner, R. W.: Geographically isolated wetlands of the United States, Wetlands, 23(3), 494–516, 2003.

Tokarz, E. and Urban, D.: SOIL REDOX POTENTIAL AND ITS IMPACT ON MICROORGANISMS AND PLANTS OF WETLANDS, Journal of Ecological Engineering, 16, 20–30, doi:10.12911/22998993/2801, 2015.

Tolić, N., Liu, Y., Liyu, A., Shen, Y., Tfaily, M. M., Kujawinski, E. B., Longnecker, K., Kuo, L.-J., Robinson, E. W., Paša-Tolić, L. and Hess, N. J.: Formularity: Software for Automated Formula Assignment of Natural and Other Organic Matter from Ultrahigh-Resolution Mass Spectra, Analytical Chemistry, 89(23), 12659–12665, doi:10.1021/acs.analchem.7b03318, 2017.

Torn, M. S., Trumbore, S. E., Chadwick, O. A., Vitousek, P. M. and Hendricks, D. M.: Mineral control of soil organic carbon storage and turnover, Nature, 389(6647), 170–173, doi:10.1038/38260, 1997.

Trettin, C. C., Laiho, R., Minkkinen, K. and Laine, J.: Influence of climate change factors on carbon dynamics in northern forested peatlands, Canadian Journal of Soil Science, 86(Special Issue), 269–280, doi:10.4141/S05-089, 2006.

Wagai, R. and Mayer, L. M.: Sorptive stabilization of organic matter in soils by hydrous iron oxides, Geochimica et Cosmochimica Acta, 71(1), 25–35, doi:10.1016/j.gca.2006.08.047, 2007.

Wang, B., Zha, T. S., Jia, X., Wu, B., Zhang, Y. Q. and Qin, S. G.: Soil moisture modifies the response of soil respiration to temperature in a desert shrub ecosystem, Biogeosciences, 11(2), 259–268, doi:10.5194/bg-11-259-2014, 2014.